

# RHEOLOGY OF CERAMIC SUSPENSIONS WITH ORGANIC OR BIOPOLYMERIC GELLING ADDITIVES PART III: SUSPENSIONS WITH STARCH

EVA GREGOROVÁ, ZUZANA ŽIVCOVÁ, WILLI PABST, JIŘI ŠTĚTINA\*, MELANIE KEUPER\*\*

*Department of Glass and Ceramics, Institute of Chemical Technology, Prague,  
Technická 5, 166 28 Prague 6, Czech Republic*

*\*Department of Dairy and Fat Technology, Institute of Chemical Technology, Prague,  
Technická 5, 166 28 Prague 6, Czech Republic*

*\*\*Institut für Geowissenschaften, Eberhardt-Karls-Universität Tübingen,  
Wilhelmstrasse 56, 72074 Tübingen, Germany*

E-mail: gregoroe@vscht.cz

Submitted March 26, 2008; accepted August 29, 2008

**Keywords:** Rheology, Relative viscosity, Suspension, Alumina, Zirconia, Starch

*In this work rotational viscometry is applied to characterize the flow behavior of starch-containing suspensions at room temperature and oscillatory shear rheometry to characterize viscoelastic behavior in dependence of the temperature. It is shown that the relative viscosity of starch suspensions in sugar solution exhibits a strongly nonlinear increase and the starch type with smallest granules, i.e. rice starch, exhibits the steepest increase of the relative viscosity with concentration. The flow curves of ceramic suspensions with corn starch exhibit characteristic differences, dependent on the ceramic powder: zirconia suspensions exhibit shear-thinning behavior even for high starch contents, while suspensions containing alumina exhibit shear-thickening behavior for significantly lower starch contents. The results of oscillatory rheometry show, that the temperature of the transition of the purely viscous suspensions with 20 vol.% starch in water to viscoelastic gels (gelatinized starch) is approx. 62°C for suspensions of potato and wheat, 68°C for rice and 71°C for corn starch suspensions. At 80°C gelatinized potato starch exhibits the highest gel strength or rigidity (storage modulus 39 kPa), while gelatinized rice starch is the weakest (approx. 9 kPa) and corn and wheat starch gels are intermediate (approx. 12 and 25 kPa, respectively). Starch-containing ceramic suspensions behave in a viscoelastic manner at room temperature and upon heating transform into purely elastic solids, with a strength (rigidity, characterized via the storage modulus) of more than 1 MPa.*

## INTRODUCTION

In the last few years starch has gained remarkable popularity as a pore-forming agent in ceramic technology [1-14], due to the lack of hygiene and ecological concerns, easy handling and processing (including defect-free burnout), the easy commercial availability in arbitrary amounts, low cost and relatively constant, controlled quality, the rounded shape with well defined aspect ratio (usually close to unity, without large scatter) and the well-defined size distribution for each starch type [15]. Apart from its universal function as a pore-forming agent, e.g. in traditional slip casting of ceramic suspensions into plaster molds, starch can serve as a body-forming agent in starch consolidation casting, due to its ability to swell in water at elevated temperatures, thus enabling ceramic green bodies to be fabricated by slip-casting of suspensions with starch into non-porous molds (e.g. metal molds) [16-26].

Starch is a natural polysaccharide (biopolymer) containing amylose and amylopectin. For basic general information on starch sources, types, composition, structure and properties the reader can refer to [15] and

the references cited therein. To a similar extent as for other new ceramic shaping techniques using organic or biopolymer additives, e.g. gelatin or carrageenan [27-31], knowledge of the viscoelastic behavior (characterized via oscillatory rheometry) is mandatory also for starch consolidation casting. However, although the rheology of starch systems is a standard theme in food science and technology [32,33], it seems that a systematic comparison of different starch types with potential interest in ceramic science and technology has never been attempted. Therefore in this paper we characterize the viscoelastic behavior of the four most important starch types to be used in ceramic shaping techniques (potato, wheat, corn and rice starch), including two examples of starch-containing alumina suspensions.

For an adequate assessment of the results presented herein and their interpretation, the reader is assumed to be familiar with the basic theory of linear viscoelasticity as outlined e.g. in the first paper (Part I) of this series [34]. Note that the viscoelastic behavior of starch systems, which exhibit a gel transition upon heating, is in certain aspects complementary to that of other gelling biopolymer systems, e.g. carrageenan systems, which

exhibit a gel transition upon cooling, cf. the second paper (Part II) of this series [31]. However, due to the fact that native starch is insoluble in water at room temperature, also the dependence of the effective suspension viscosity on the starch content is of interest for ceramic processing (in traditional slip casting, where starch is used as a mere pore-forming agent, as well as in starch consolidation casting, where starch is used as a combined pore-forming and body-forming agent), since it determines the flow behavior during the casting step. Therefore, results of measurements by rotational viscometry are included in the present investigation as well.

### THEORETICAL

Native starch is a natural biopolymer composite consisting of an essentially linear polysaccharide (amylose, see Figure 1) with molecular weight of the order of  $10^5$ - $10^6$  and a highly branched polysaccharide (amylopectin, see Figure 2) with molecular weight of the order of  $10^7$ - $10^9$ , usually in combination with small amounts of proteins and lipids. The density of completely dry starch is approx.  $1.6 \text{ g/cm}^3$ , but at the equilibrium moisture content (between approx. 15 and 20 % for cereal and potato starch, respectively) it is reduced to approx.  $1.5 \text{ g/cm}^3$ . About 70 wt.% of a starch granule is regarded as amorphous (amylose and amylopectin) and 30 wt.% as crystalline (mainly amylopectin). Amylose can be dissolved or leached from the starch granules without disrupting them and without disturbing the crystalline character. The degree of crystallinity depends on the water content. Most starches contain between 20 and 30 wt.% amylose. Special starch types, however, contain much more amylose (e.g. amylo maize starch with 60-70 % amylose), while other types are essentially amylose-free (e.g. "waxy" corn starch with only 5 % amylose). The reader may refer to [32,33,35] for more detailed information. It is known that after dissolution in water the intrinsic viscosity  $[\eta]$  of macro-

molecular polymer solutions, i.e. the first order coefficient in their viscosity concentration dependence, measured under isothermal conditions, follows a power law of the form

$$[\eta] = K \cdot M^N \quad (1)$$

(Mark-Houwink relation), where  $M$  is the molecular weight and  $K$  and  $N$  are fit parameters [36]. It should therefore be expected that the viscosity increase due to amylopectin is higher than that due to amylose. On the other hand, while amylose will be leached out of the starch granules and dissolves in water at rather low temperatures ( $60$ - $70^\circ\text{C}$ ) during swelling, amylopectin can leave the starch granules only after disintegration of the granules and skin rupture, leading to irreversible gelatinization of the starch-water mixture. That means, amylopectin can contribute to a viscosity increase only when it can freely diffuse in the suspension. In starch consolidation casting of ceramic suspensions, however, this free diffusion of amylopectin is greatly impeded by the ceramic powder present (excluded volume effect), and therefore the role of amylopectin for the body formation step in this process is certainly only a minor one.

Concerning the interpretation of measured stress response data in terms of linear viscoelasticity the reader is referred to Part I of this series [34]. In particular, it has to be remembered that viscoelastic systems in small amplitude oscillatory shear are characterized by a complex modulus

$$G^* = G' + iG'' \quad (2)$$

where  $G'$  is the storage modulus,  $G''$  the loss modulus and the loss factor (damping factor, loss tangent) is given by

$$\tan \delta = G''/G' \quad (3)$$

where  $\delta$  is the phase shift (phase angle) and  $\delta = 90^\circ$  corresponds to purely viscous behavior and  $\delta = 0^\circ$  to purely elastic behavior. Recall also that the loss modulus (i.e. the imaginary part of the complex modulus) is

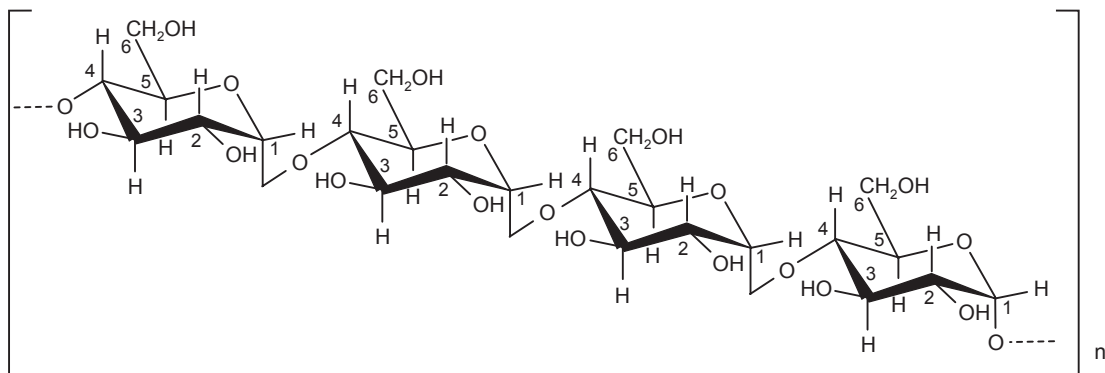


Figure 1. Amylose.

related to the viscosity (real part of the complex viscosity) via the relation

$$G'' = \omega \eta', \quad (4)$$

where  $\omega$  is the angular frequency [30-34].

At room temperature up to the onset of swelling (at temperatures higher than approx. 60°C), the starch granules present in the suspension can be treated as rigid particles and therefore the effective (apparent) viscosity of the suspension is a function of the volume fraction of starch. Theoretical model relations describing the dependence of the relative viscosity on the volume fraction of dispersed particles have been reviewed in [37]. In particular, it has to be recalled that in the dilute limit the relative viscosity  $\eta_r = \eta/\eta_0$  is linearly dependent on the solids volume fraction function  $\phi$  according to the Einstein-Jeffery relation [38-40]

$$\eta_r = 1 + [\eta]\phi, \quad (5)$$

where  $[\eta]$  is the intrinsic viscosity and that the concentration dependence of nondilute and concentrated suspensions can be fitted using the Krieger relation [38,41] in the form

$$\eta_r = \left(1 - \frac{\phi}{\phi_{\max}}\right)^{-[\eta]\phi_{\max}}, \quad (6)$$

where  $\phi_{\max}$  is the maximum volume fraction which can be introduced into the suspension without blocking (clogging), i.e. the solids volume fraction at which the system ceases to be fluid. Theoretically, it may be determined as an asymptotic value by fitting measured relative viscosity data (for an appropriately wide viscosity range) in dependence of the volume fraction. A slightly

more restricted special case of the Krieger relation is the empirical Maron-Pierce relation [38,42],

$$\eta_r = \left(1 - \frac{\phi}{\phi_c}\right)^{-2}, \quad (7)$$

which has the practical advantage of being a one-parameter relation, with the empirical fit parameter (critical volume fraction), which has to be interpreted as a relative measure for the maximally attainable volume fraction when the viscosity range measured is limited.

## EXPERIMENTAL

### Material characteristics and sample preparation

The starch types used in this work are potato starch (Solamyl, Naturamyl, Czech Republic), wheat starch (Amylon, Czech Republic), corn starch (Gustin, Dr. Oetker, Czech Republic and Amioca TF, National Starch & Chemical, Germany) and rice starch (Remy Industries, Belgium), see the particle size distributions in Figure 3. For rotational viscometry starch suspensions with starch contents in the range 10-30 vol.% (based on an average starch density of 1.5 g/cm<sup>3</sup>) were prepared in 60 wt.% sugar (saccharose) solutions (with density 1.285 g/cm<sup>3</sup> and viscosity 50 mPas at 23°C) by agitating with alumina balls for 1 h. For oscillatory rheometry suspensions with 20 vol.% starch were prepared in distilled water, also by agitating with alumina balls for 1 h. The sugar solution in the first case served to avoid sedimentation effects and to shift the viscosities to higher absolute values for a more precise deter-

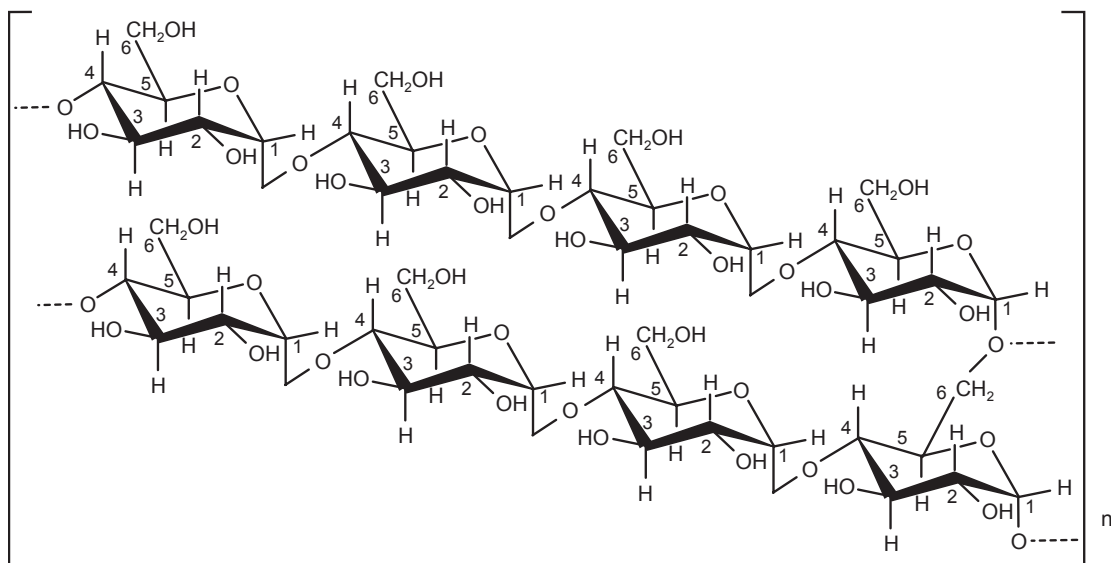


Figure 2. Amylopectin.

mination of the relative viscosities, while in order to characterize the temperature dependence of the rheological behavior (including swelling and gelatinization) pure water had been used in order to avoid starch-sugar interactions.

Three types of submicron-sized ceramic powders have been used in this work: alumina (CT-3000 SG, Almatix, Germany; average particle size 0.8  $\mu\text{m}$ , specific surface approx. 7  $\text{m}^2/\text{g}$ ), zirconia (TZ-3YE, Tosoh, Japan; average crystallite size 40 nm, with a secondary particle size of a few hundred nm, specific surface approx. 16  $\text{m}^2/\text{g}$ ) and a zirconia-based composite powder with 20 wt.% alumina (ATZ-80, Daiichi-Kigenso, Japan; average particle size 0.3  $\mu\text{m}$ , specific surface approx. 15  $\text{m}^2/\text{g}$ ). Ceramic suspensions were prepared with 1 wt.% (related to the ceramic powder) deflocu-

lant (Dolapix CE 64, Zschimmer & Schwarz, Germany) by agitating for 1 h and ultrasonication. For the preparation of starch-containing suspensions the starch was added to the ceramic powder before suspending the powder mix in water. Alumina suspensions were prepared either with potato starch or with corn starch (Gustin), zirconia and zirconia-based suspensions only with corn starch (Amioca TF).

#### Measurement details

Viscometric measurements at room temperature ( $23 \pm 1^\circ\text{C}$ ) were performed using a rotational viscometer (RotioVisco 1, Haake, Germany) with a coaxial cylinder sensor (Z 41, gap 3 mm) in the shear rate range between 0 and 1000  $\text{s}^{-1}$ . The measurements were performed in a stepwise mode (with 30 s data acquisition at each 100  $\text{s}^{-1}$  step) with an upward and downward ramp.

Small amplitude oscillatory shear measurements, to characterize the viscoelastic response of the systems and their temperature dependence, were performed using an oscillatory rheometer (RheoStress 80, Haake, Germany) with a coaxial cylinder sensor system (Z 40, gap 8 mm), connected to a thermostatic heater (DC 30). A cover plate was used to prevent evaporation and to guarantee uniform heating. An oscillation frequency of 1 Hz and a heating rate of  $3^\circ\text{C}/\text{min}$  has been applied throughout.

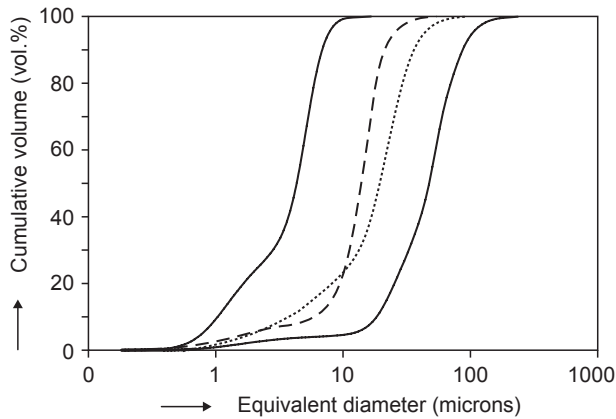


Figure 3. Comparison of size distributions of starch granules (from left to right: rice starch/full curve, corn starch/dashed curve, wheat starch/dotted curve, and potato starch/full curve).

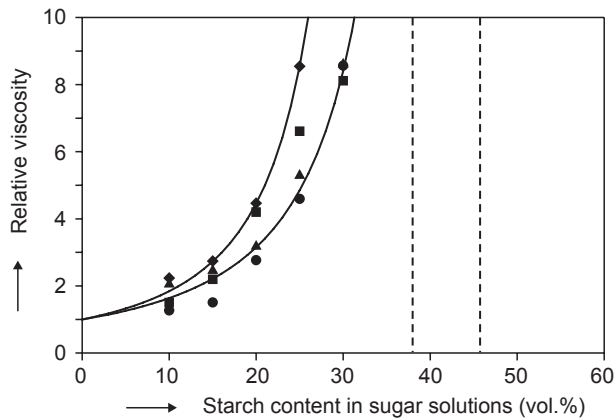


Figure 4. Relative viscosity of starch suspensions in 60 wt.% sugar solutions in dependence of the starch volume fraction; experimentally determined data points (rice starch/diamonds, corn starch/squares, wheat starch/triangles, potato starch/circles), fitted curves (full curves, for rice starch on the l.h.s., for potato starch on the r.h.s.) and extrapolated critical volume fractions (vertical lines, for rice starch on the l.h.s., for potato starch on the r.h.s.).

## RESULTS AND DISCUSSION

Suspensions of starch (density approx.  $1.5 \text{ g}/\text{cm}^3$ ) in 60 wt.% sugar solutions (density  $1.285 \text{ g}/\text{cm}^3$  and viscosity 49 mPas at  $23^\circ\text{C}$ ), measured by rotational viscometry at room temperature, exhibit almost Newtonian behavior in the range of starch contents investigated (10-30 vol.%), except for rice starch, where a slight tendency to shear-thinning and thixotropy could be observed for contents more than 20 vol.%. Figure 4 shows the relative viscosity of starch suspensions in dependence of the starch volume fraction. Fitting these results with the Maron-Pierce relation, Equation (7), yields  $\phi_c$  values between 0.38 (for rice starch suspensions) and 0.46 (for potato starch suspensions), which indicates that with starch types of larger particle size higher volume fractions can be attained in suspensions of comparable viscosity. As expected, the corresponding values for wheat and corn starch are intermediate, in accordance with their intermediate particle size.

When starch is added to a ceramic suspension, the situation is principally similar: the starch granules increase the viscosity. However, the situation is complicated by the fact that ceramic suspensions with starch

exhibit non-Newtonian behavior, as shown in Figures 5 to 7: alumina and ATZ suspensions are shear-thickening (dilatant), while zirconia suspensions are shear-thinning (pseudoplastic). The probable reason for this remarkable difference in flow behavior is that the zirconia consists of submicron-sized agglomerates or secondary particles (a few hundred nanometers in size) of nano-sized primary particles (size < 100 nm), while the alumina (including the alumina contained in the ATZ powder) consists of primary particles with a size of approx. 0.8  $\mu\text{m}$ . Under high-shear conditions the submicron zirconia secondary particles (agglomerates) can disintegrate into smaller entities, while the submicron alumina particles cannot.

Figure 8 shows the relative viscosity of alumina, ATZ and zirconia suspensions (calculated as the ratio of the effective apparent viscosity of the starch-containing ceramic suspension at a shear rate of 500  $\text{s}^{-1}$  and the viscosity of the starch-free ceramic suspension) in dependence of the starch content in the suspensions (cf. Tables 1-3). Fitting with the Maron-Pierce relation gives  $\phi$  values between 0.23 and 0.34, which is significantly

lower than for starch suspensions without ceramic powder (cf. Figure 4 and the discussion above), obviously due to the fact that the presence of the ceramic powder, in addition to starch, leads to excluded volume effects.

Figure 9 shows the apparent viscosity of the starch-containing ceramic suspensions versus the total solids content (i.e. ceramic powder and starch granules). It is evident that the pure alumina suspensions have a much higher solids content than the zirconia-based suspensions. This solids content is essentially determined by the ceramic powder content of the base suspensions, which is 50 vol.% for alumina and approx. 30 % in the zirconia-based suspensions at comparable viscosity levels. This difference, a well-known empirical finding, is due to the fact that zirconia powder has a higher specific surface area (viz. 16  $\text{m}^2/\text{g}$  versus 7.5  $\text{m}^2/\text{g}$  for alumina, corresponding to surface densities of approx. 100  $\text{m}^2/\text{cm}^3$  versus 30  $\text{m}^2/\text{cm}^3$  for alumina). Therefore, more water is immobilized in the form of adsorbed layers around the particles and the tendency to agglomeration is higher (and thus water is additionally immobilized within the agglomerates).

Table 1. Apparent and relative viscosities of 80 wt.% alumina (CT-3000 SG, Almatix) suspensions with different contents of corn starch.

Nominal starch content (vol.%)	Starch content in suspension (vol.%)	Total solids content in suspension (vol.%)	$\eta_{500}$ (mPas)	$\eta_{1000}$ (mPas)	$\eta_r$ (at 500/s)
0	0	50	49	50	1
5	2.6	51.3	86	96	1.8 - 1.9
10	5.3	52.6	129	145	2.6 - 2.9
15	8.1	54.1	149	170	3.0 - 3.4
20	11.1	55.6	156	214	3.2 - 4.3
25	14.3	57.1	190	254	3.9 - 5.0
30	17.6	58.8	295	–	6.0

Table 2. Apparent and relative viscosities of 70 wt.% zirconia-alumina (ATZ-80, Daiichi) suspensions with different contents of corn starch.

Nominal starch content (vol.%)	Starch content in suspension (vol.%)	Total solids content in suspension (vol.%)	$\eta_{500}$ (mPas)	$\eta_{1000}$ (mPas)	$\eta_r$ (at 500/s)
0	0	29.7	50	47	1
6	1.9	31.1	63	61	1.3
18	6.1	34.1	87	100	1.7 - 2.1
24	8.6	35.8	123	147	2.5 - 3.1
36	14.3	39.8	342	–	7.0

Table 3. Apparent and relative viscosities of 70 wt.% zirconia (TZ-3YE, Tosoh) suspensions with different contents of corn starch.

Nominal starch content (vol.%)	Starch content in suspension (vol.%)	Total solids content in suspension (vol.%)	$\eta_{500}$ (mPas)	$\eta_{1000}$ (mPas)	$\eta_r$ (at 500/s)
0	0	27.7	44	34	1
5	1.4	28.7	48	40	1.1 - 1.2
15	4.7	31.1	58	46	1.3 - 1.4
20	6.5	32.4	111	81	2.4 - 2.5
40	15.6	39.0	142	103	3.1 - 3.2
45	18.5	41.1	217	150	4.5 - 4.9

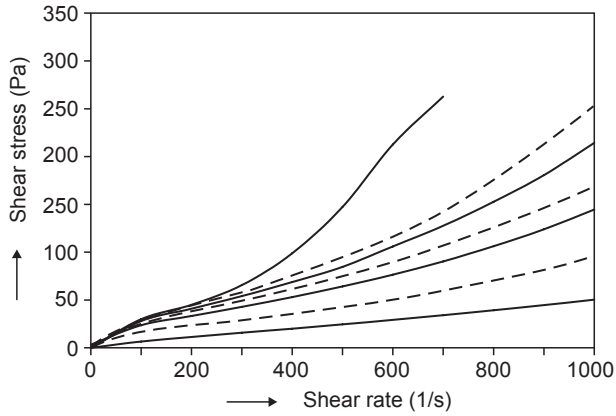


Figure 5. Flow curves of 80 wt.% alumina suspensions with (from bottom to top) 0, 5, 10, 15, 20, 25 and 30 vol.% of corn starch (related to ceramic powder) at room temperature.

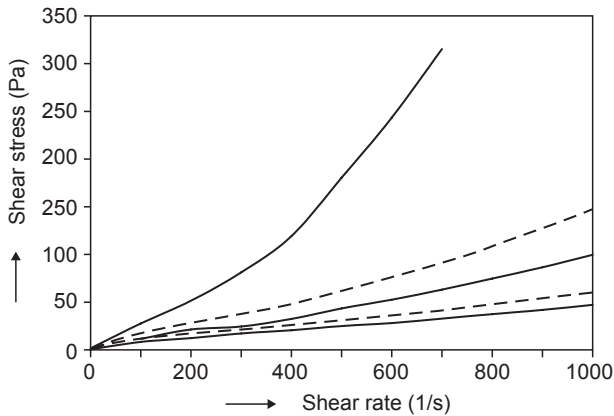


Figure 6. Flow curves of 70 wt.% ATZ suspensions with (from bottom to top) 0, 6, 18, 24 and 36 vol.% of corn starch (related to ceramic powder) at room temperature.

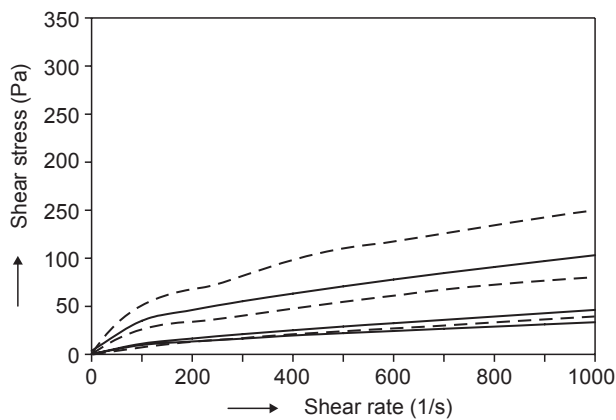


Figure 7. Flow curves of 70 wt.% zirconia suspensions with (from bottom to top) 0, 5, 15, 20, 40 and 45 vol.% of corn starch (related to ceramic powder) at room temperature.

Figures 10 and 11 show the behavior of starch-in-water suspensions with 20 vol.% starch in dependence of the temperature during heating up from room temperature. The ordinates on the l.h.s. refer to the storage modulus  $G'$  and loss modulus  $G''$ , on the r.h.s. to the phase shift  $\delta$ . It can be seen that at room temperature all suspensions are purely viscous (i.e. the phase shift is  $90^\circ$ ), independent of the starch type, with viscosities in the range 10-100 mPas for rice and corn starch (Figure 10) and 100-1000 mPas for wheat and potato starch (Figure 11). With increasing temperature the viscosity is slightly increasing (note the logarithmic scale), due to the swelling of the starch granules. At temperatures higher than approx.  $60^\circ\text{C}$  gelatinization occurs,

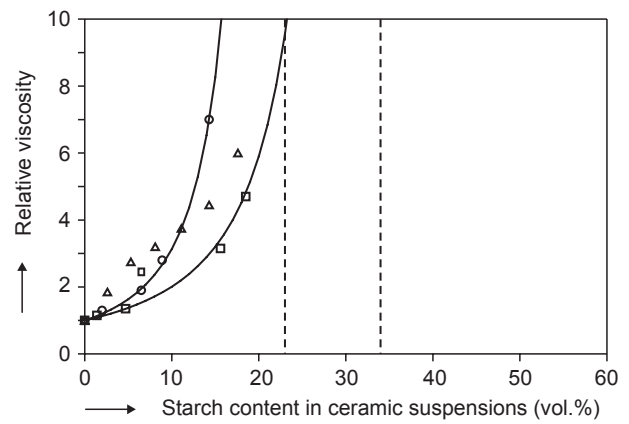


Figure 8. Relative viscosity (at  $500\text{ s}^{-1}$ ) of corn-starch-containing ceramic suspensions in dependence of the starch volume fraction; experimentally determined data points (alumina suspensions/triangles, zirconia-alumina suspensions/circles, zirconia suspensions/squares), fitted curves (full curves, for zirconia-alumina suspensions on the l.h.s., for zirconia suspensions on the r.h.s.) and extrapolated critical volume fractions (vertical lines, for zirconia-alumina suspensions on the l.h.s., for zirconia suspensions on the r.h.s.).

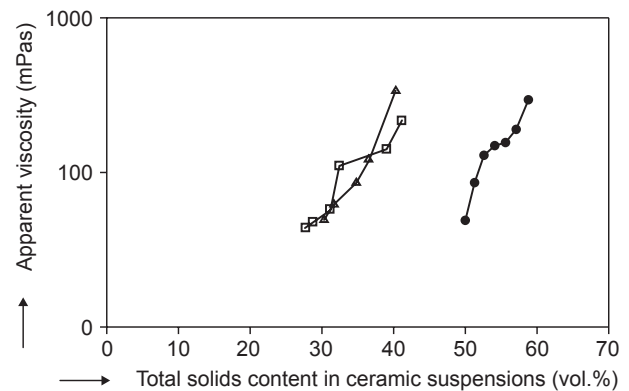


Figure 9. Apparent viscosity at  $500\text{ s}^{-1}$  versus total solids content (ceramic powder and starch) in suspensions at room temperature ( $23^\circ\text{C}$ ): alumina (circles), ATZ (triangles), zirconia (squares).

accompanied by the onset of viscoelastic behavior and the appearance of a finite value for the storage modulus. This gelatinization temperature is 68°C for rice starch, 71°C for corn starch (cf. Figure 10) and approx. 62°C for wheat and potato starch (Figure 11), in good agreement with literature values [15,36]. At 80°C the starch gel formed from potato starch is the strongest ( $G' = 39$  kPa) and that formed from rice starch the weakest ( $G' = 9$  kPa). Corn and wheat starch are intermediate in this respect (approx. 12 and 25 kPa, respectively).

Figures 12 and 13 shows the temperature dependence of the storage modulus and the phase shift of starch-containing alumina suspensions. It is evident that even at low temperature (40°C) these suspensions are viscoelastic (phase shift in the range 10-70°C) and not purely viscous as in the case without ceramic powder. Upon heating these suspensions undergo a transition to a purely elastic body (phase shift 0°), with the transition temperature evidently determined by the starch type (59°C for potato starch, cf. Figure 12, and 73°C for corn starch, cf. Figure 13). In both cases the high storage

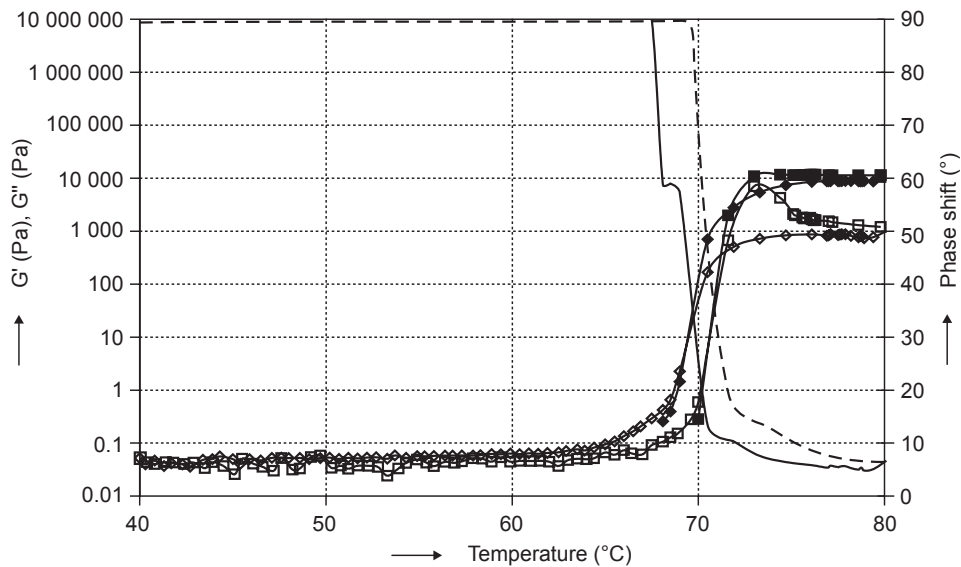


Figure 10. Temperature dependence of the storage modulus (bold curves with full symbols), loss modulus (thin curves with empty symbols) and phase shift (curves without symbols) for aqueous suspensions with 20 vol.% starch: rice starch (diamonds and full phase shift curve) and corn starch (squares and dashed phase shift curve).

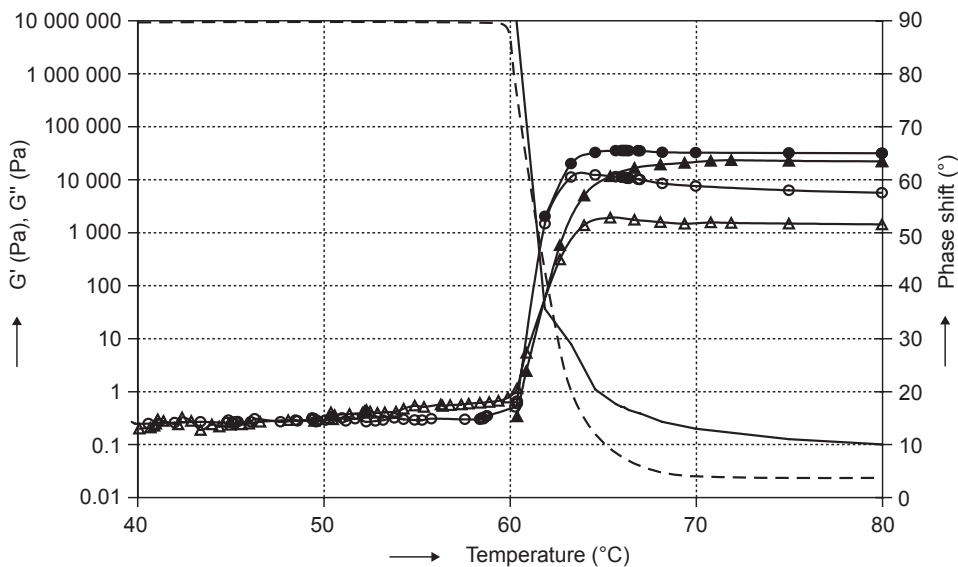


Figure 11. Temperature dependence of the storage modulus (bold curves with full symbols), loss modulus (thin curves with empty symbols) and phase shift (curves without symbols) for aqueous suspensions with 20 vol.% starch: wheat starch (triangles and dotted phase shift curve) and potato starch (circles and full phase shift curve).



modulus (1.5 MPa and 1.1 MPa, respectively) corresponds to the high strength of alumina ceramic green bodies prepared by starch consolidation casting. This strength is higher than that of carrageenan-cast alumina bodies [30,31] by approx. 2 orders of magnitude.

### SUMMARY AND CONCLUSIONS

In this work rotational viscometry has been applied to characterize the flow behavior of starch-containing suspensions at room temperature and oscillatory shear

rheometry to characterize viscoelastic behavior in dependence of the temperature. It has been shown that the relative viscosity of starch suspensions in sugar solution exhibits a strongly nonlinear increase, which can be fitted using the Maron-Pierce relation, resulting in critical volume fractions of starch between 0.38 and 0.46 (as expected, the starch type with smallest granules, i.e. rice starch, exhibits the steepest increase of the relative viscosity with concentration).

The flow curves of ceramic suspensions with corn starch exhibit characteristic differences, dependent on

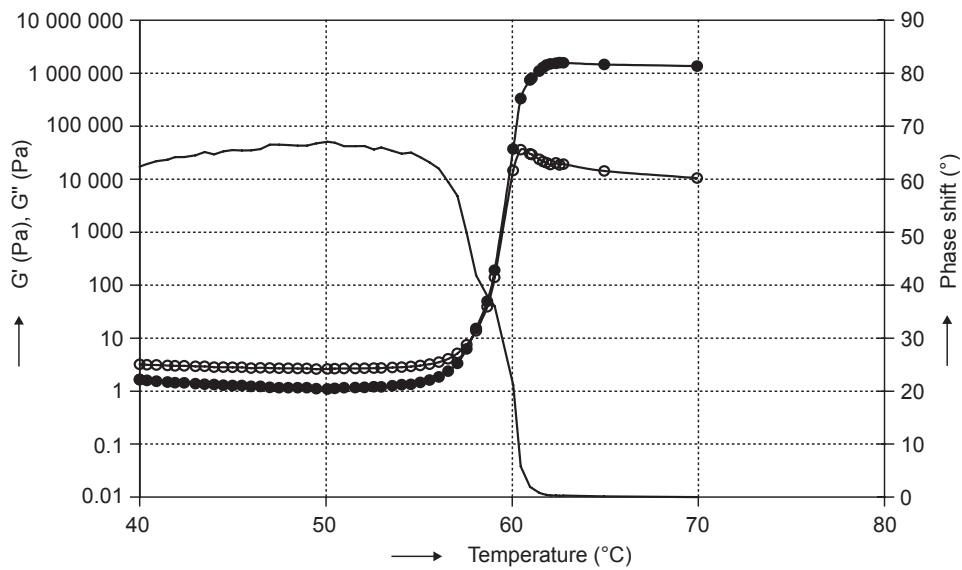


Figure 12. Temperature dependence of the storage modulus (bold curves with full symbols), loss modulus (thin curves with empty symbols) and phase shift (curves without symbols) for a 70 wt.% alumina suspension with 30 vol.% potato starch (related to ceramic powder).

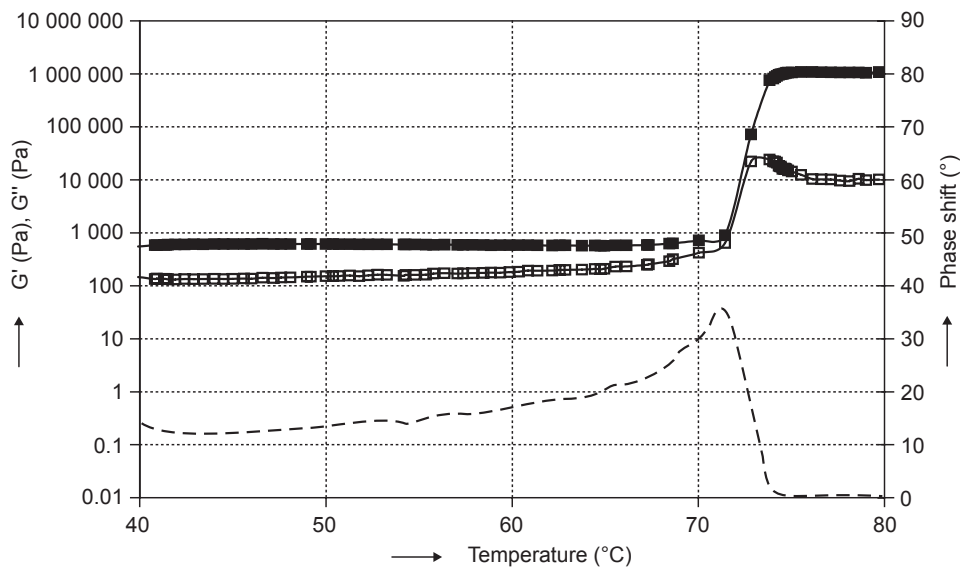


Figure 13. Temperature dependence of the storage modulus (bold curves with full symbols), loss modulus (thin curves with empty symbols) and phase shift (curves without symbols) for a 80 wt.% alumina suspension with 20 vol.% corn starch (related to ceramic powder).



the ceramic powder. Suspensions of ZrO<sub>2</sub> (70 wt.% Tosoh TZ-3YE) exhibit shear-thinning (pseudoplastic) behavior even for nominal starch contents (i.e. starch contents related to the ceramic power) of 45 vol.% (corresponding to 18.5 vol.% of starch or 41 vol.% of ZrO<sub>2</sub> and starch in the suspension). On the other hand, suspensions containing Al<sub>2</sub>O<sub>3</sub> (either pure alumina Almatis CT-3000 SG, or composite powder ZrO<sub>2</sub>-Al<sub>2</sub>O<sub>3</sub> with a prevalence of ZrO<sub>2</sub>, i.e. Daiichi-Kigensu ATZ-80) exhibit shear-thickening (dilatant) behavior for significantly lower starch contents. Thus, the viscometric measurements show that from the viewpoint of rheology the highest starch content without negative consequences on the fluidity can be achieved in zirconia suspensions with the starch type of largest granule size (potato starch). It has to be remembered, however, that for viscosities of the same order of magnitude the overall content of ceramic phase is significantly higher with alumina suspensions (50 vol.% alumina) than for zirconia suspensions (with only approx. 30 vol.% zirconia). This is also reflected in the well-known fact that the shrinkage of slip-cast zirconia bodies is always significantly higher than that of slip-cast alumina bodies.

The results of oscillatory rheometry show, that the temperature of the transition of the purely viscous suspensions with 20 vol.% starch in water to viscoelastic gels (gelatinized starch) is approx. 62°C for suspensions of potato and wheat starch, 68°C for rice starch and 71°C for corn starch suspensions. At 80 °C gelatinized potato starch exhibits the highest gel strength or rigidity (storage modulus 39 kPa), while gelatinized rice starch is the weakest (approx. 9 kPa) and corn and wheat starch gels are intermediate (approx. 12 and 25 kPa, respectively). Starch-containing ceramic suspensions behave in a viscoelastic manner already at room temperature (phase shift 10-70°) and upon heating transform into purely elastic solids (phase shift 0°), as soon as the temperature corresponding to starch gelatinization is exceeded (approx. 59°C for the suspension containing potato starch and 73°C for the suspension containing corn starch). The strength (rigidity) of these solids, characterized via the storage modulus, is 1.5 and 1.1 MPa, respectively, which is approx. two orders of magnitude higher than the gel strength of ceramic bodies made by other gelcasting techniques, e.g. using carrageenan.

#### Acknowledgement

*This work was part of the research project "Preparation and Research of Functional Materials and Material Technologies using Micro- and Nanoscopic Methods", supported by the Ministry of Education, Youth and Sports of the Czech Republic (Grant No. MSM 6046137302). The stay of M.K. at the ICT Prague was supported by the DAAD - AVČR grant No. D2 - CZ 21/06-07.*

#### References

1. Corbin S. F., Apte P. S.: *J. Am. Ceram. Soc.* **82**, 1693 (1999).
2. Davis J., Kristoffersson A., Carlström E., Clegg W.: *J. Am. Ceram. Soc.* **83**, 2369 (2000).
3. Galassi C., Roncari E., Capiati C., Fabbri G., Piancastelli A., Peselli M., Silvano F.: *Ferroelectrics* **268**, 47 (2002).
4. Kim J. G., Sim J. H., Cho W.: *J. Phys. Chem. Solids* **63**, 2079 (2002).
5. Kim J. G., Cho W. S., Sim J. H.: *J. Mater. Sci. - Mater. Electr.* **13**, 497 (2002).
6. Díaz A., Hampshire S.: *J. Eur. Ceram. Soc.* **24**, 413 (2004).
7. Mattern A., Huchler B., Staudenecker D., Oberacker R., Nagel A., Hoffmann M. J.: *J. Eur. Ceram. Soc.* **24**, 3399 (2004).
8. Reynaud C., Thévenot F., Chartier T., Besson J.-L.: *J. Eur. Ceram. Soc.*, **25**, 589 (2005).
9. Barea R., Osendi M. I., Ferreira J. M. F., Miranzo P.: *Acta Mater.* **53**, 3313 (2005).
10. Galassi C.: *J. Eur. Ceram. Soc.* **26**, 2951 (2006).
11. García-Gabaldón M., Pérez-Herranz V., Sánchez E., Mestre S.: *J. Membrane Sci.* **280**, 536 (2006).
12. Studart A.R., Gonzenbach T., Tervoort E., Gauckler, L. J.: *J. Am. Ceram. Soc.* **89**, 1771 (2006).
13. Gregorová E., Živcová Z., Pabst, W.: *J. Mater. Sci.* **41**, 6119 (2006).
14. Živcová Z., Gregorová E., Pabst, W.: *Proc. Appl. Ceram.* **2**, 1-8 (2008).
15. Gregorová E., Pabst W., Bohačenko, I.: *J. Eur. Ceram. Soc.* **26**, 1301 (2006).
16. Lyckfeldt O., Ferreira J. M. F.: *J. Eur. Ceram. Soc.* **18**, 131 (1998).
17. Alves H. M., Tari G., Fonseca A. T., Ferreira J. M. F.: *Mater. Res. Bull.* **33**, 1439 (1998).
18. Lemos A.F., Ferreira J. M. F.: *Mater. Sci. Eng. C11*, 35 (2000).
19. Bowden M. E., Rippey M. S.: *Key Eng. Mater.* **206-213**, 1957 (2002).
20. Romano P., Velasco F. J., Torralba J. M., Candela N.: *Mater. Sci. Eng. A* **419**, 1 (2006).
21. LeBeau J. M., Boonyongmaneerat Y.: *Mater. Sci. Eng. A* **458**, 17 (2007).
22. Yang L., Ning X., Chen K., Zhou, H.: *Ceram. Intern.* **33**, 483 (2007).
23. Sopyan I., Mel M., Ramesh S., Khalid K. A.: *Sci. Technol. Adv. Mater.* **8**, 116 (2007).
24. Gregorová E., Pabst W.: *J. Eur. Ceram. Soc.* **27**, 669 (2007).
25. Bhattacharjee S., Besra L., Singh B. P.: *J. Eur. Ceram. Soc.* **27**, 47 (2007).
26. Mao X., Wang S., Shimai S.: *Ceram. Intern.* **34**, 107 (2008).
27. Olhero S. M., Tari G., Coimbra M. A., Ferreira, J. M. F.: *J. Eur. Ceram. Soc.* **20**, 423 (2000).
28. Santacruz I., Nieto M. I., Moreno R.: *J. Am. Ceram. Soc.* **85**, 2432 (2002).
29. Ortega F. S., Valenzuela F. A. O., Scuracchio C. H., Pandolfelli V. C.: *J. Eur. Ceram. Soc.* **23**, 75 (2003).
30. Gregorová E., Pabst W., Štětina J.: *J. Eur. Ceram. Soc.* **26**, 1185 (2006).
31. Gregorová E., Pabst W., Štětina J.: *Ceramics-Silikaty* **50**, 232 (2006).
32. Biliaderis C. G.: *Structures and phase transitions of starch polymers*, in: *Polysaccharide Association Structures in Food*, p.57-168, Ed. Walter R.H., Marcel Dekker, New York 1998.

33. Okechukwu P. E., Rao M. A.: *Rheology of structured polysaccharide food systems - starch and pectin*, in: Polysaccharide Association Structures in Food, p.289-328, Ed. Walter R. H., Marcel Dekker, New York 1998.
34. Gregorová E., Pabst W., Štětina J.: *Ceramics-Silikaty* 48, 93 (2004).
35. Belitz H. D., Grosch W., Schieberle P.: *Food Chemistry* (3<sup>rd</sup> edition), p.298-341, Springer Verlag, Berlin 2004.
36. Owusu-Apenten R. K.: *Introduction to Food Chemistry*, p.51-54 and p.123-140, CRC Press, Boca Raton 2005.
37. Pabst W.: *Ceramics-Silikaty* 48, 6 (2004).
38. Pabst W., Gregorová E., Berthold C.: *J. Eur. Ceram. Soc.* 26, 149 (2006).
39. Einstein A.: *Ann. Physik* 19, 289 (1906).
40. Jeffery G. B.: *Proc. Roy. Soc. Lond. A* 102, 161 (1922).
41. Krieger I. M.: *Adv. Colloid Interface Sci.* 3, 111 (1972).
42. Maron S. H., Pierce P. E.: *J. Colloid Sci.* 11, 80 (1956).

REOLOGIE KERAMICKÝCH SUSPENZÍ S OBSAHEM ORGANICKÝCH RESP. BIOPOLYMERNÝCH GELUJÍCÍCH ADITIV  
ČÁST III: SUSPENZE S OBSAHEM ŠKROBU

EVA GREGOROVÁ, ZUZANA ŽIVCOVÁ,  
WILLI PABST, JIŘI ŠTĚTINA\*, MELANIE KEUPER\*\*

*Ústav skla a keramiky,  
Vysoká škola chemicko-technologická v Praze,  
Technická 5, 166 28 Praha 6  
\*Ústav technologie mléka a tuků,  
Vysoká škola chemicko-technologická v Praze,  
Technická 5, 166 28 Praha 6  
\*\*Institut für Geowissenschaften,  
Eberhard-Karls-Universität Tübingen,  
Wilhelmstrasse 56, 72074 Tübingen, SRN*

V keramické technologii roste v souvislosti s novými tvarovacími metodami keramických suspenzí zájem i o reologii vodných soustav s obsahem škrobů, včetně jejich viskoelastického chování. Přítomnost nativního škrobu v keramické suspenzi se projevuje vždy zvýšením viskozity, protože škrob je při pokojové teplotě ve vodě nerozpustný. Škrob může mít v keramické technologii dvojí funkci: funkci pórotvorného činidla a funkci tělesotvorného činidla; v obou případech zůstává konečný keramický výrobek po výpalu porézni. Funkce škrobu jakožto tělesotvorné přísady v procesu tzv. škrobového lití je založena na schopnosti škrobu bobtnat ve vodě při zvýšené teplotě a tím absorbovat vodu z okolní suspenze. Růst objemu škrobových zrn pak způsobí stlačení keramických částic do prostoru mezi škrobová zrna. Při teplotách nad cca. 60°C dochází po krátkém čase k mazovatění, tj. zpočátku čistě viskózní suspenze se mění ve viskoelastickou soustavu. V tomto článku je pomocí rotační viskozimetrie charakterizováno tokové chování škrobových suspenzí při pokojové teplotě a pomocí oscilační reometrie jejich viskoelastické vlastnosti v závislosti na teplotě. Je ukázáno, že relativní viskozita škrobových suspenzí v cukerném roztoku vykazuje silně nelineární

nárůst, který lze proložit Kriegerovým resp. Maron-Piercovým vztahem s kritickou objemovou frakcí 0.38-0.46, přičemž nejmenší škrob (tj. rýžový) vykazuje nejstrmější nárůst se vzrůstající koncentrací. Keramické suspenze s obsahem škrobu vykazují charakteristické rozdíly v tokových křivkách: suspenze ZrO<sub>2</sub> (70 hmot.% Tosoh TZ-3YE) vykazují pseudoplastické chování ještě pro nominální obsah škrobu 45 obj.% (vztaženo na ZrO<sub>2</sub>, tzn. 18.5 obj.% škrobu v suspenzi resp. 41 obj.% ZrO<sub>2</sub> + škrob v suspenzi), zatímco suspenze s obsahem Al<sub>2</sub>O<sub>3</sub> (jak čistého korundu Almatix CT-3000 SG, tak kompozitního prášku ZrO<sub>2</sub>-Al<sub>2</sub>O<sub>3</sub> s převahou ZrO<sub>2</sub>, tj. Daiichi-Kigenso ATZ-80) vykazují již při výrazně nižším obsahu škrobu dilatantní chování. Viskozimetrická měření při pokojové teplotě tedy ukazují, že z hlediska reologie lze nejvyššího obsahu škrobu bez negativního dopadu na lící vlastnosti (tekutost) suspenzí docílit u suspenzí ZrO<sub>2</sub> při použití škrobu větších velikostí, např. bramborového. Je však důležité mít na zřeteli, že při řádově stejné viskozitě je celkový obsah keramické fáze výrazně větší u korundových suspenzí (50 obj.% Al<sub>2</sub>O<sub>3</sub>, oproti cca. 30 obj.% v suspenzích na bázi ZrO<sub>2</sub>), s čímž souvisí známá skutečnost, že smrštění litých těles na bázi ZrO<sub>2</sub> je vždy výrazně větší než smrštění litých těles Al<sub>2</sub>O<sub>3</sub>. Výsledky měření oscilační reometrií ukazují, že teplota přechodu čistě viskózních suspenzí (s 20 obj.% škrobu) na viskoelastické gely resp. mazy je cca. 62°C pro vodní suspenze bramborového a pšeničného škrobu, 68°C pro suspenze rýžového a 71 °C pro suspenze kukuřičného škrobu. Při teplotě 80°C se jeví gel (maz) bramborového škrobu jako nejtuzší (akumulační modul 39 kPa), rýžový maz jako nejméně tuhý (cca. 9 kPa). Kukuřičný a pšeničný maz jsou uprostřed (cca. 12 resp. 25 kPa). Keramické suspenze s obsahem škrobu se chovají jako viskoelastické soustavy (charakterizovány fázovým posunem v rozsahu 10-70°) již při nízké teplotě a při zahřátí na teplotu mazovatění škrobu (která odpovídá přibližně teplotě naměřené pro škrobové suspenze bez keramických prášků, tj. 59°C pro suspenze s bramborovým škrobem a 73°C pro suspenze s kukuřičným škrobem) se přeměňují na víceméně čistě elastická pevná tělesa. Pevnost těchto těles, charakterizována akumulacním modulem, je 1.5 resp. 1.1 MPa, což je řádově vyšší než pevnost těles získaných např. karagenovým litím.